Pergamon International Journal of Machine Tools & Manufacture 41 (2001) 1165–1188

INTERNATIONAL JOURNAL OF MACHINE TOOLS & MANUFACTURE DESIGN, RESEARCH AND APPLICATION

Effects of support misalignments in deep-hole drill shafts on hole straightness

Chyn-Shu Deng, Jen-Chen Huang, Jih-Hua Chin *

Department of Mechanical Engineering, National Chiao Tung University, Hsinchu, Taiwan, ROC

Received 15 March 2000; received in revised form 4 January 2001; accepted 8 January 2001

Abstract

This work investigates the effect of drill shaft support misalignment on hole straightness in relation to the various control factors. Misalignments occur in machine spindles, intermediate supports and pilot bushings. Equations for axial hole straightness deviation are derived herein using the Euler column theory, and experiments are performed using Gundrill and BTA deep-hole drilling systems. Simulation results, Sakuma's method and experimental examinations are also presented. Taguchi methods and statistical techniques are used to formulate the experimental layout, analyze the effect of each control factor on the results, and optimize the setting for each control factor. Further experiments then verify these estimates. Six control factors were used in a modified L8 orthogonal array design. The confirmatory experiments revealed an average straightness deviation within the 95% confidence interval. © 2001 Published by Elsevier Science Ltd.

Keywords: Deep-hole drilling; Support misalignment; Hole straightness deviation control factors

1. Introduction

Deep-hole drilling, defined as when the ratio of hole-depth to hole-diameter exceeds ten, produces holes of accurate size, roundness, straightness and surface finish. However, the dynamics of the long drill shaft influence the drilling process so that the deflection caused by the lateral bending and vibration of the deep-hole drill shaft compromises the hole straightness. To suppress the deflection and thus enhance hole straightness, pilot bushing and intermediate support are used to stabilize the long drill shaft in deep-hole drilling. However, the assembly accuracy of pilot bushing, intermediate support and machine spindle in turn significantly influence the dynamics.

* Corresponding author. Tel.: +886-35-731-965; fax: +886-35-727-485.
E-mail address: jhchin@cc.nctu.edu.tw (J.-H. Chin).

0890-6955/01/$ - see front matter © 2001 Published by Elsevier Science Ltd.
PII: S0890-6955(01)00007-4

Nomenclature

d : Tool diameter, mm
d_o : Outer diameter of drill shaft, mm
d_i : Inner diameter of drill shaft, mm
E : Young's modulus of drill shaft, GPa
e_n : Level of hole straightness deviation in arbitrary depth X_n, mm
I : Cross-sectional area moment of inertia of drill shaft, m^4
L : Drill shaft length, mm
ℓ_1 : Distance from spindle to intermediate support location, mm
n : Total revolutions of drill shaft, $n=X_n/\Delta X$
P : Axial thrust force, N
Q,R : Reaction force, N
ΔX : Feed rate, mm/rev
X_n : Penetration depth, mm
ρ : Mass density of drill shaft, kg/m^3
δ_B, δ_S : Misalignments of the pilot bushing and intermediate support, respectively, mm
y,y_1,y_2 : Deflection function
y,y_2',y_2' : Slope function
M,M_1,M_2 : Moment function
DF : Degrees of freedom
SS : Sum of squares
V' : Mean square
F : Fisher statistic
SS′ : Pure sum of squares
P′ : Percentage contribution, %

For example, the misaligned pilot bushing or drill shaft support compromises the straightness of the drilled hole. This paper investigates as to how the pilot bushing and intermediate support misalignments affect hole straightness.

Frazao et al. [1] described the merits of a novel three-pad BTA tool over the conventional two-pad BTA tools. They experimentally verified that the three-pad BTA tool was more stable than conventional BTA tools during deep-hole drilling. The third pad also stiffens the tool, thereby enhancing the chip-breaking performance and improving the quality of holes produced at high feed rates. Sakuma et al. [2] developed formulas representing the burnishing action of guide pads and also studied the over-size mechanism of a machined hole. Sakuma et al. [3] investigated the effects of guide pads on the burnishing action and accuracy of machined holes using a uniquely designed tool. Meanwhile, the formation mechanism of multi-corner shaped holes was also considered. The burnishing action on the hole wall and the self-guiding action of the tool were examined by Sakuma et al. [4]. Sakuma et al. also considered the effects of pilot bushing and intermediate support misalignments on hole straightness, but did not consider the axial thrust forces, i.e. hole deviation was completely dependent upon the drill shaft geometrical parameters

in the model (see Appendix B). Further, Rao and Shunmugam [5] analyzed the axial and transverse profiles of holes obtained from BTA drilling, and Katsuki et al. [6] studied the influence of workpiece geometry on the axial hole deviation in deep-hole drilling. Katsuki et al. [7] investigated the role of single- and multi-edge tools in hole deviation. Their experimental data and theoretical analyses suggested that tool geometry imbalanced the cutting forces and caused hole deviations. Katsuki et al. also investigated how an inclined workpiece front face and pre-drilled pilot holes affected the hole deviation. Hole deviations were found to vary with wall thickness between adjacent holes and with the diameters of pre-drilled pilot holes. Meanwhile, parallel hole deviations increased with the pilot hole diameter, and hole deviations rose sharply when the thickness of the wall separating adjacent holes reached a certain value. Stuerenburg [8] studied hole deviation during single-lip deep-hole drilling using an experimental approach, ignoring the theoretical considerations.

Hole straightness deviations in deep-hole drilling are affected by the tool diameter, feed rate, shaft length, distance from spindle to intermediate support location, and misalignments of pilot bushing and intermediate support. This study focuses on investigating the effects of misalignments of pilot bushing and intermediate supports of deep-hole drill shafts subjected to various factors controlling hole straightness. The equations for hole straightness deviation were derived using the Euler column theory. Meanwhile, experiments were performed using Gundrill and BTA deep-hole drilling systems. Simulation results, Sakuma's method [4] and experimental results were also compared. For optimum efficiency in the planning and analysis of experimental data, Taguchi's [9–13] parameter design was applied to investigate the multi-variate process, and the signal-to-noise ratio (S/N) response was calculated. The results were verified by conducting a few trial runs under optimum conditions.

2. Equations for hole straightness deviation

Fig. 1 illustrates the drill shaft support misalignment during deep-hole drilling. Although Sakuma et al. [4] also considered the misalignment during deep-hole drilling, they however concen-

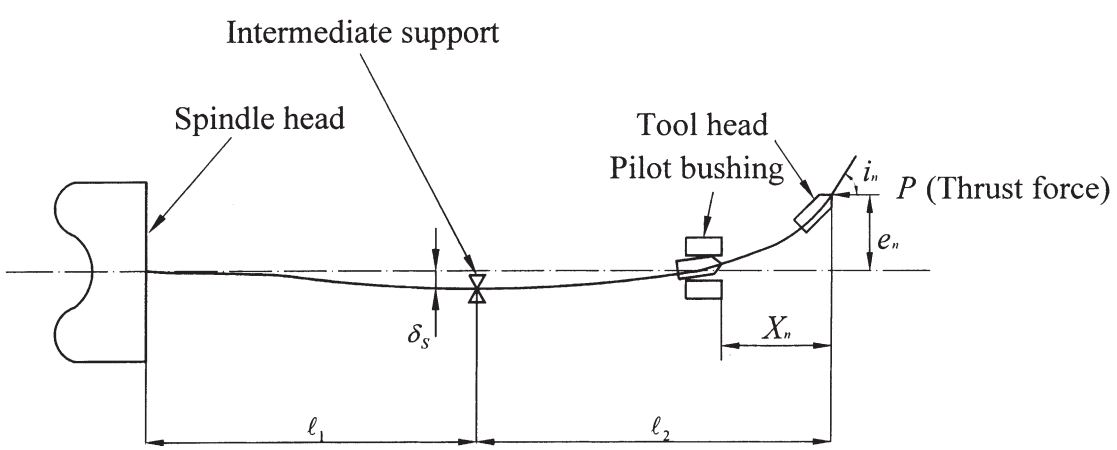

Fig. 1. Drill shaft support misalignment in deep-hole drilling.

trated mainly on geometry as their analysis considered no other parameters, such as thrust forces acting on the drill shafts, and Young's modulus of the drill shaft.

Equations for hole straightness deviations owing to misalignments of pilot bushing and intermediate drill shaft supports are derived below.

2.1. Equation for hole straightness deviation due to pilot bushing misalignment

To minimize the deflection and enhance hole straightness, a pilot bushing is used to stabilize the long drill shaft in deep-hole drilling. If the pilot bushing is inclined or laterally displaced, the tool head is forced away from the spindle axis, as illustrated in Fig. 2.

The lateral deviation becomes increasingly pronounced with feed movement as the tool head penetrates the workpieces. Typical hole straightness deviations at arbitrary depths may be expressed mathematically as

$$e_n = e_{n-1} + i_{n-1}\Delta X \tag{1}$$

where e_n denotes the amount of deviation of hole at arbitrary depth X_n, ΔX represents the feed rate, n ($n = X_n/\Delta X$) is the total revolutions of the drill shaft, X_n denotes the penetrated depth, and i_{n-1} represents the inclination of the deflected drill shaft after $(n-1)$ revolutions. Notably, Eq. (1) is valid for small drill deflections, which apply in practical deep-hole drilling.

Assume that the pilot bushing misalignment is δ_B (Fig. 2). When the tool head penetrates the workpiece, the thrust force begins to affect the inclination of the drill head. The inclination produced by thrust force P during an incremental movement of ΔX conforms to the Euler column theory [14]. Fig. 3 presents a moment diagram of the drill shaft with pilot bushing misalignment.

During drilling, the moment at (x,y), $M(x,y)$, along the drill shaft is given by the following expression:

$$M(x,y) = P(\delta_B - y) + Q(L - x) \tag{2}$$

Since the deflection is small compared to the shaft length, the following relation holds:

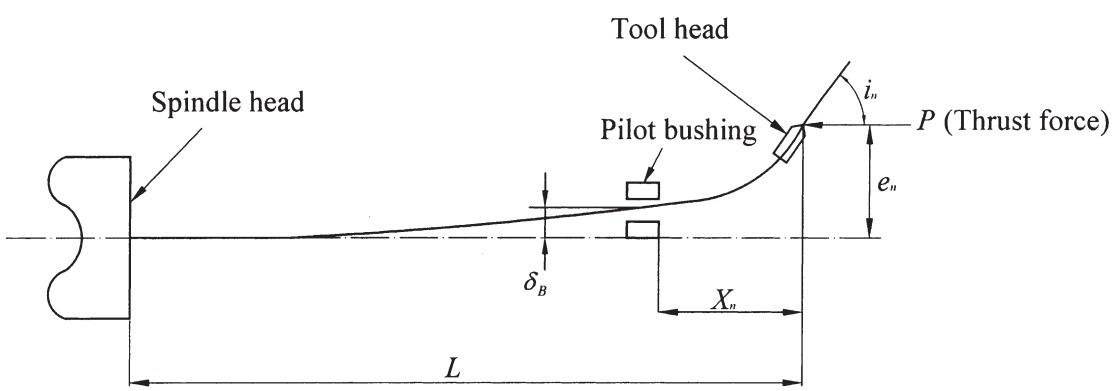

Fig. 2. Pilot bushing misalignment.

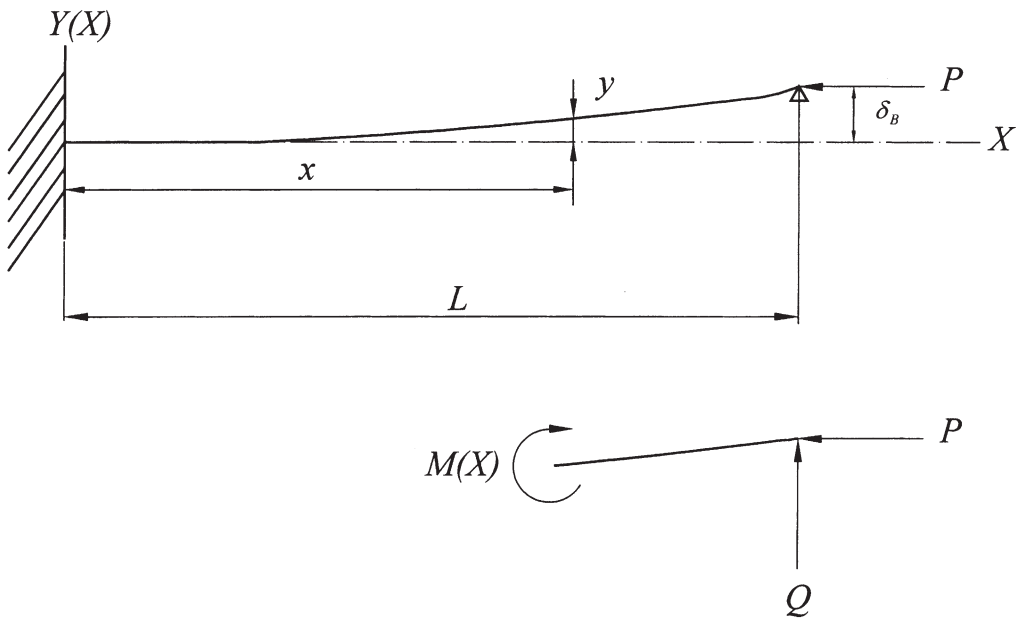

Fig. 3. Moment diagram of drill shaft pilot bushing misalignment.

$$M=EI\frac{d^2y}{dx^2} \tag{3}$$

Thus, the drill shaft deflection can be described by

$$EI\frac{d^2y}{dx^2}=P(\delta_B-y)+Q(L-x) \tag{4}$$

with the boundary conditions

$$y(0)=0 \quad y'(0)=0 \quad y(L)=\delta_B \tag{5}$$

Eq. (4) can be rewritten in the form

$$\frac{d^2y}{dx^2}+\lambda^2y=\lambda^2\left(\delta_B+\frac{Q}{P}(L-x)\right) \tag{6}$$

where

$$\lambda=\sqrt{\frac{P}{EI}} \tag{7}$$

where P is the thrust force; E the Young's modulus of drilling tool shaft; and I the second moment of area of drilling tool shaft:

$$I=\frac{\pi(d_o^4-d_i^4)}{64} \text{ for BTA drilling; } I=\frac{I_{XX}+I_{YY}}{2} \text{ for Gun drilling}$$

The general solution of Eq. (6) is

$$y(x)=U\cos\lambda x+V\sin\lambda x+\delta_{\mathrm{B}}+\frac{Q}{P}(L-x) \tag{8}$$

where U and V are constants.

Applying the boundary conditions given by Eq. (5), yields the constants as

$$U=-\frac{\sin\lambda L}{\sin\lambda L-L\lambda\cos\lambda L}\delta_{\mathrm{B}} \text{ and } V=-\frac{\cos\lambda L}{\sin\lambda L-L\lambda\cos\lambda L}\delta_{\mathrm{B}} \tag{9}$$

It can also be shown that

$$Q=\frac{P\lambda\cos\lambda L}{\sin\lambda L-L\lambda\cos\lambda L}\delta_{\mathrm{B}}$$

The drill shaft inclination equation is a first-order derivative of $y(x)$, in other words,

$$y'(x)=-U\lambda\sin\lambda x+V\lambda\cos\lambda x-\frac{Q}{P} \tag{10}$$

The initial drill head inclination i_0 is given by

$$i_0=y'(L)=\frac{\lambda(1-\cos\lambda L)}{\sin\lambda L-L\lambda\cos\lambda L}\delta_{\mathrm{B}} \tag{11}$$

Meanwhile, the drill head deviation after penetration ΔX is

$$e_1=i_0\Delta X+\delta_B=\left[1+\frac{\lambda(1-\cos\lambda L)}{\sin\lambda L-L\lambda\cos\lambda L}\Delta X\right]\delta_{\mathrm{B}} \tag{12}$$

Thus, deviation e_n at hole depth X_n is

$$e_n=\left[1+\frac{\lambda(1-\cos\lambda L)}{\sin\lambda L-L\lambda\cos\lambda L}\Delta X\right]^n\delta_{\mathrm{B}} \tag{13}$$

The simple equation presented by Sakuma et al. [4] (Eq. (B1)) excluded the effect of the drilling tool shaft being subjected to thrust force and bending, and also excluded other parameters such as tool diameter, Young's modulus of the drill shaft, and so on. Eq. (13) includes all these considerations, and thus describes the hole deviation caused by pilot bushing δ_{B} misalignment during deep-hole drilling better.

2.2. Equation of hole straightness deviation due to intermediate support misalignment

Fig. 1 displays the misalignment of a drill shaft intermediate support. The moment on the drill shaft is because of the deflection from misalignment, as illustrated in Fig. 4. The misalignment at the location of intermediate support is assumed to be δ_B.

The moment equations for the intervals $0 \le x \le \ell_1$ and $\ell_1 \le x \le L$ are

$$M_1(x) = P(\delta_B - y) + Q(L-x) - R(\ell_1 - x) \quad 0 \le x \le \ell_1 \tag{14}$$

$$M_2(x) = P(\delta_B - y) + Q(L-x) \quad \ell_1 \le x \le L \tag{15}$$

Thus, the differential equations governing the drill shaft deflections are

$$EI\frac{d^2y_1}{dx^2} = P(\delta_B - y) + Q(L-x) - R(\ell_1 - x) \quad 0 \le x \le \ell_1 \tag{16}$$

$$EI\frac{d^2y_2}{dx^2} P(\delta_B - y) + Q(L-x) \quad \ell_1 \le x \le L \tag{17}$$

with boundary conditions

$$y_1(0) = 0 \; y_1(\ell_1) = y_2(\ell_1) = -\delta_S \; y_2(L) = \delta_B$$

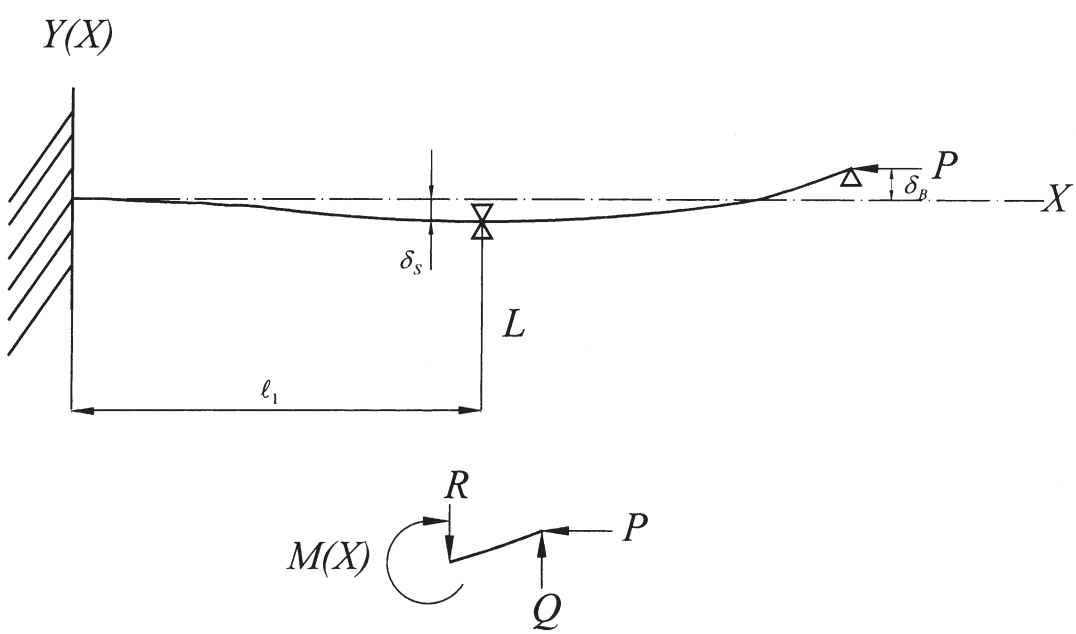

Fig. 4. Moment diagram of drill shaft intermediate support misalignment.

$$y'_1(0)=0 \quad y'_1(\ell_1)=y'_2(\ell_1) \tag{18}$$

Eqs. (16) and (17) can be rewritten in the form

$$\frac{d^2y_1}{dx^2}+\lambda^2 y_1=\lambda^2\left(\delta_B+\frac{Q}{P}(L-x)-\frac{R}{P}(\ell_1-x)\right) \quad 0\le x\le \ell_1 \tag{19}$$

$$\frac{d^2y_2}{dx^2}+\lambda^2 y_2=\lambda^2\left(\delta_B+\frac{Q}{P}(L-x)\right) \quad \ell_1\le x\le L \tag{20}$$

where parameter λ is defined as in Eq. (7).

The general solutions for Eqs. (19) and (20) are

$$y_1(x)=U_1\cos\lambda x+V_1\sin\lambda x+\delta_B+\frac{Q}{P}(L-x)-\frac{R}{P}(\ell_1-x) \quad 0\le x\le \ell_1 \tag{21}$$

$$y_2(x)=U_2\cos\lambda x+V_2\sin\lambda x+\delta_B+\frac{Q}{P}(L-x) \quad \ell_1\le x\le L \tag{22}$$

Applying the boundary conditions given by Eq. (18) produces a number of equations presented in matrix form below

$$\begin{bmatrix} 1 & 0 & 0 & 0 & L/P & -\ell_1/P \\ 0 & \lambda & 0 & 0 & -1/P & 1/P \\ \cos\lambda\ell_1 & \sin\lambda\ell_1 & 0 & 0 & (L-\ell_1)/P & 0 \\ 0 & 0 & \cos\lambda\ell_1 & \sin\lambda\ell_1 & (L-\ell_1)/P & 0 \\ 0 & 0 & \cos\lambda L & \sin\lambda L & 0 & 0 \\ -\lambda\sin\lambda\ell_1 & \lambda\cos\lambda\ell_1 & \lambda\sin\lambda\ell_1 & -\lambda\cos\lambda\ell_1 & 0 & 1/P \end{bmatrix} \begin{bmatrix} U_1 \\ V_1 \\ U_2 \\ V_2 \\ Q \\ R \end{bmatrix} = \begin{bmatrix} -\delta_B \\ 0 \\ -\delta_S-\delta_B \\ -\delta_S-\delta_B \\ 0 \\ 0 \end{bmatrix} \tag{23}$$

or expressed in the compact matrix form

$$\mathbf{AB}=\mathbf{C} \tag{24}$$

The solution of coefficient matrix **B** is

$$\mathbf{B}=\mathbf{A}^{-1}\mathbf{C} \tag{25}$$

The equation for the drill shaft inclination for the interval $\ell_1 \leq x \leq L$ is

$$y'_2(x) = -U_2\lambda \sin \lambda x + V_2\lambda \cos \lambda x - \frac{Q}{P} \quad \ell_1 \leq x \leq L \tag{26}$$

Therefore, the inclination i_0 of the tool head is

$$i_0 = y_2(L) \tag{27}$$

The deviation of the tool head after penetration ΔX is

$$e_1 = i_0 \Delta X + e_0 \tag{28}$$

Thus, the tool head deviation e_n along the axial direction at penetration depths X_n can be obtained using the iterative method. Eq. (28) can also be applied to predict hole straightness deviations accurately when both the intermediate support and pilot bushing are misaligned. Fig. 5 shows a flow chart for determining the results of intermediate support and pilot bushing misalignments.

3. Experiments and results

3.1. Experimental setup

This study focused on the hole deviation caused by misalignments under various control factors. A series of experiments were performed on a modified machine which can accommodate both BTA deep-hole drilling and Gun drilling to examine the effects of pilot bushing and drill shaft intermediate support misalignments on hole straightness.

Fig. 6(a) displays the BTA drilling machine. The machine has an external cutting fluid supply and internal chip transport. The tool head is screwed onto the drilling tube. Cutting fluid is supplied through the space between the drilling tube and the machined hole, and then removed along with the chips through the drill tube. The cross-section of the drill shaft is round, making it much more rigid than the Gundrill shaft.

Fig. 6(b) shows the gun drilling machine. The Gun drill consists of a single-lip drill head of cemented carbide, and a shaft with an internal duct for cutting fluid. The cutting fluid is supplied through the duct inside the drill, and flushes out from the front flank of the cutting edge. Chip transport takes place externally in a V-shaped chip flute on the drill shaft.

3.2. Workpiece material

The workpiece material was AISI 1020 steel, of 60 mm×100 mm and 250 mm in length. The workpiece was drilled to a depth of 220 mm and cut into four pieces (50 mm length) after the drilling test. The deviation was measured over a length of 200 mm. Fig. 7 shows a sample of the sectioned workpiece.

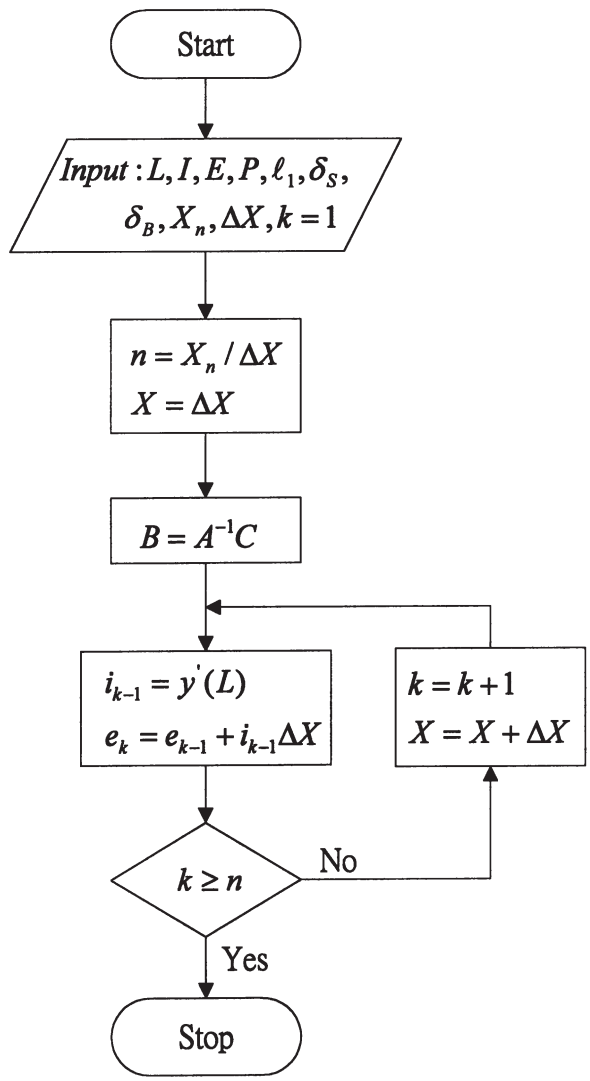

Fig. 5. Flow chart for calculating the effects of drill shaft intermediate support and pilot bushing misalignments.

3.3. Measurement of the machine setup

Fig. 8 shows the setup for measuring the tool thrust during drilling. Force signals detected by a dynamometer were transferred to the strain amplifiers that converted the voltage signals into force values. The data acquisition system (microlink) acquired dynamic force signals from the strain amplifiers and saved them in static memories (SRAM). The acquired data were processed and analyzed to establish an empirical model of thrust forces using MATHEMATICA software. The empirical equations for thrust force can be used to calculate thrust forces for different conditions when drilling the same material.

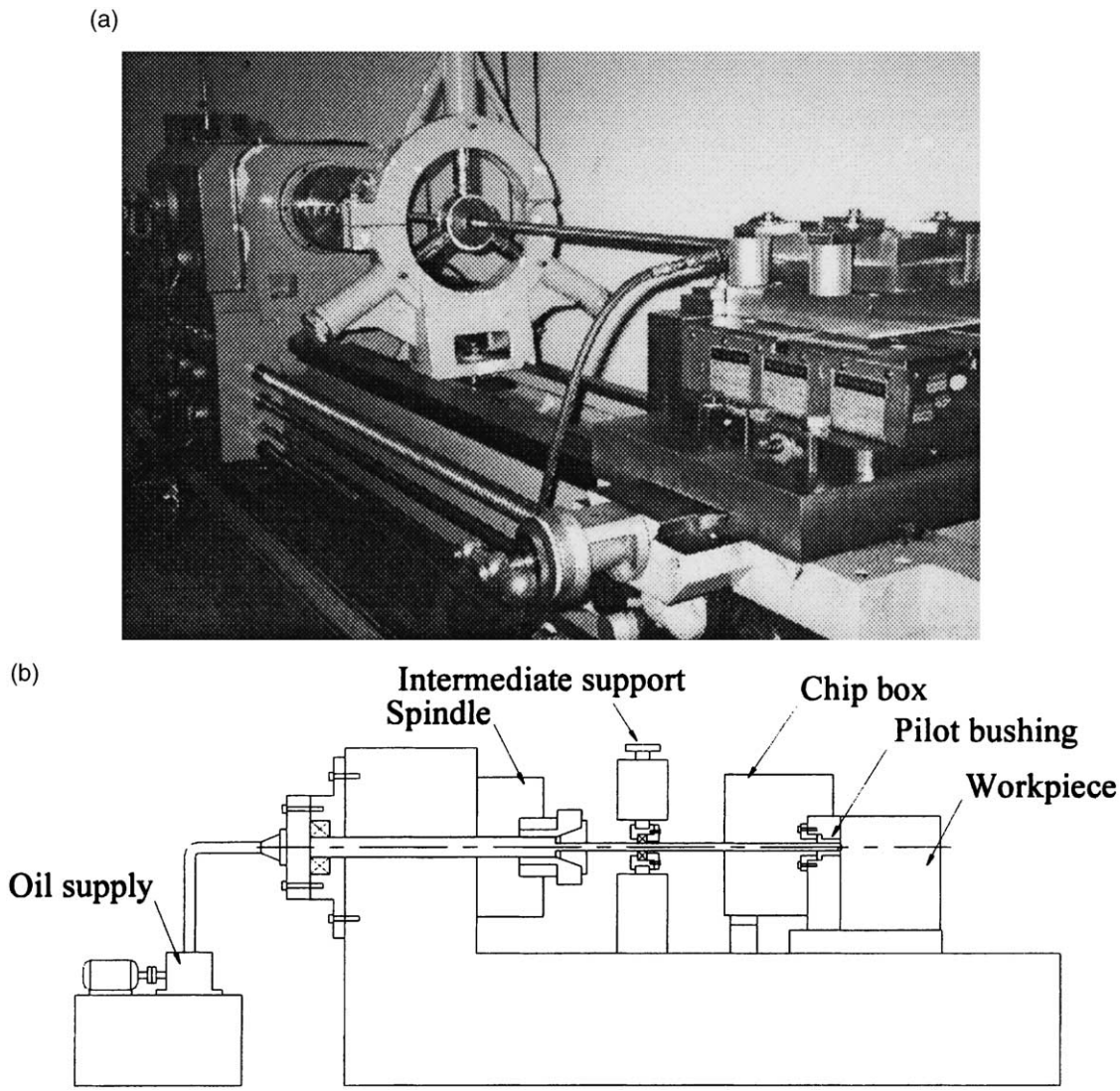

Fig. 6. (a) BTA drilling system. (b) Gun drilling system.

3.4. Empirical modelling of thrust forces

The experimental machining was performed at a rotational speed of 585 rpm. Drilling tests were carried out for the BTA and the Gun drilling systems, respectively. The machining conditions were:

feed rates: 0.05–0.10 mm/rev
tool diameters for BTA drilling system: 18.91, 19.90, 24.11, 26.40 mm
tool diameters for Gun drilling system: 8.02, 9.52, 11.52, 12.52 mm

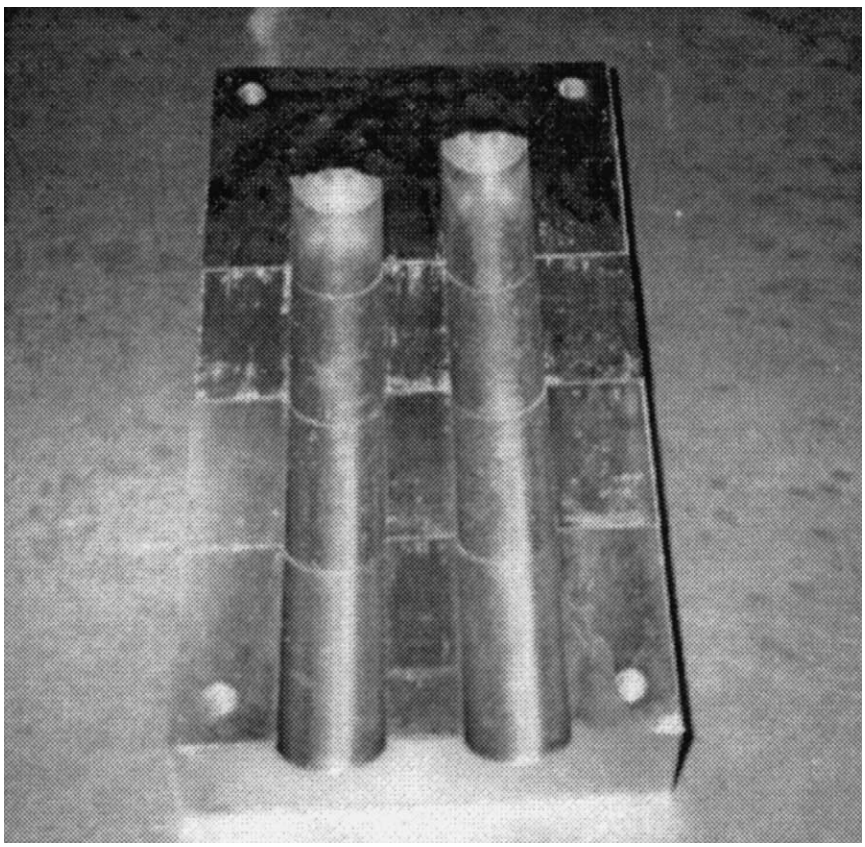

Fig. 7. Workpiece product.

Table 1 gives the second moment of areas about the x–x and y–y axes for the Gun drills used [8]. Meanwhile, Table 2(a) lists the mean and RMS thrust force values with respect to feed rate and tool diameter for BTA deep-hole drilling, while Table 2(b) lists the same for Gun drilling, respectively. Empirical equations for estimating thrust were obtained as Eqs. (29a) and (29b).

$$P = 838.614 \Delta X^{0.957} d^{0.981} \quad \text{for BTA drilling} \tag{29a}$$

$$P = 423.136 \Delta X^{0.399} d^{0.545} \quad \text{for Gun drilling} \tag{29b}$$

These empirically obtained thrust values (P) were used later in the simulation equations (7) and (23)

3.5. Experimental analysis

Fig. 9(a) shows the influence of the length of various BTA drill shafts on hole straightness deviation. Meanwhile, Fig. 9(b) shows the corresponding results for Gun drilling. The drilling

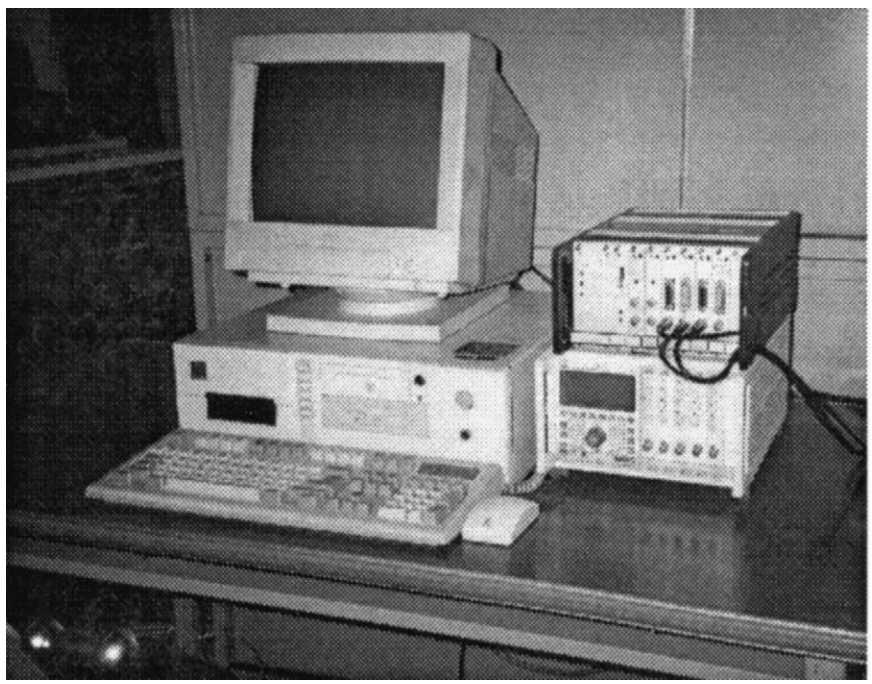

Fig. 8. Experimental setup for measuring tool thrust force.

Table 1
Gun drilling second moment of area

Tool shaft diameter	0.00802 m	0.00952 m	0.01152 m	0.01252 m
Total length of tool shaft (L)	0.640 m	0.640 m	0.840 m 1.115 m	0.840 m 1.115 m
Second moment of area about the y-axis (I_{xx})	0.780×10^{10} m^4	1.859×10^{10} m^4	3.172×10^{10} m^4	4.487×10^{10} m^4
Second moment of area about the z-axis (I_{yy})	1.171×10^{10} m^4	2.926×10^{10} m^4	4.870×10^{10} m^4	6.829×10^{10} m^4

shafts were subjected to a pilot bushing misalignment of 0.1 mm for BTA drilling, and an intermediate support misalignment of 0.1 mm for Gun drilling. Interestingly, for both the BTA and the Gun drill, the shorter drill shaft yielded larger straightness deflections. This phenomenon can be explained by Eq. (30) where the drill head slope i_0 for the shorter drill shaft is larger than that for the longer drill shaft.

$$i_0=\frac{\delta_B}{L} \tag{30}$$

The overall straightness deflection increases with deflection slope as the shaft penetrates the workpiece. Eq. (1) illustrates that axial hole straightness deviation increases with the drill head

Table 2
BTA drilling and Gun drilling mean thrust force (unit: N)

Tool diameter (mm)	Feed rate (mm/rev)	Mean thrust force	Root mean square
(a) *BTA drilling*			
18.91	0.05	783.011	782.885
	0.07	1156.961	1157.125
	0.10	1699.058	1699.398
19.90	0.05	936.526	937.767
	0.07	1220.298	1221.480
	0.10	1866.680	1868.478
24.11	0.05	1087.912	1088.843
	0.07	1390.192	1390.607
	0.10	2113.804	2113.541
26.40	0.05	1289.280	1290.369
	0.07	1615.308	1616.101
	0.10	2174.281	2175.405
(b) *Gun drilling*			
8.02	0.06	404.948	405.599
	0.08	473.266	474.064
	0.10	576.061	576.994
9.52	0.06	476.554	477.796
	0.08	520.482	521.557
	0.10	563.534	562.550
11.52	0.06	525.639	526.317
	0.08	561.354	562.550
	0.10	614.756	614.994
12.52	0.06	574.600	574.863
	0.08	622.331	622.935
	0.10	667.180	667.608

slope i_0. Three results, the predicted value, experimental value and Sakuma predicted value, were compared. Figs. 9–11 reveal that the proposed models (Eqs. (13) and (28)) give more accurate results than the Sakuma equation. The accuracy of these models derives by taking into consideration more of the factors involved in the drilling. Sakuma's model (Eqs. (B1) and (B2)) considered the shaft diameter d, shaft length L, distance from the spindle to the intermediate support location ℓ_1, and feed rate ΔX, and misalignment δ_S, δ_B. In addition to the above variables, the proposed model considers the drilling thrust P, Young's modulus of the shaft material E, and the moment of inertia of the shaft I. Fig. 10(a) illustrates the influence of thrust P in BTA drilling on straightness deviation, while Fig. 10(b) shows the corresponding results for Gun drilling. The compressive axial force (thrust force) applied to drill shafts tends to lower the natural frequencies [15] because it reduces the effective shaft stiffness. When the axial thrust P increases, the drill head slope i_n also might increase, along with the hole straightness deviation. In Sakuma's model the straightness deviation was independent of axial thrust force. Fig. 11(a) and (b) shows the influence of the distance from spindle to intermediate support location (ℓ_1) on the axial hole straightness deviation. Fig. 11(a) displays the axial hole straightness deviation for pilot bushing misalignment of 0.1 *mm*,

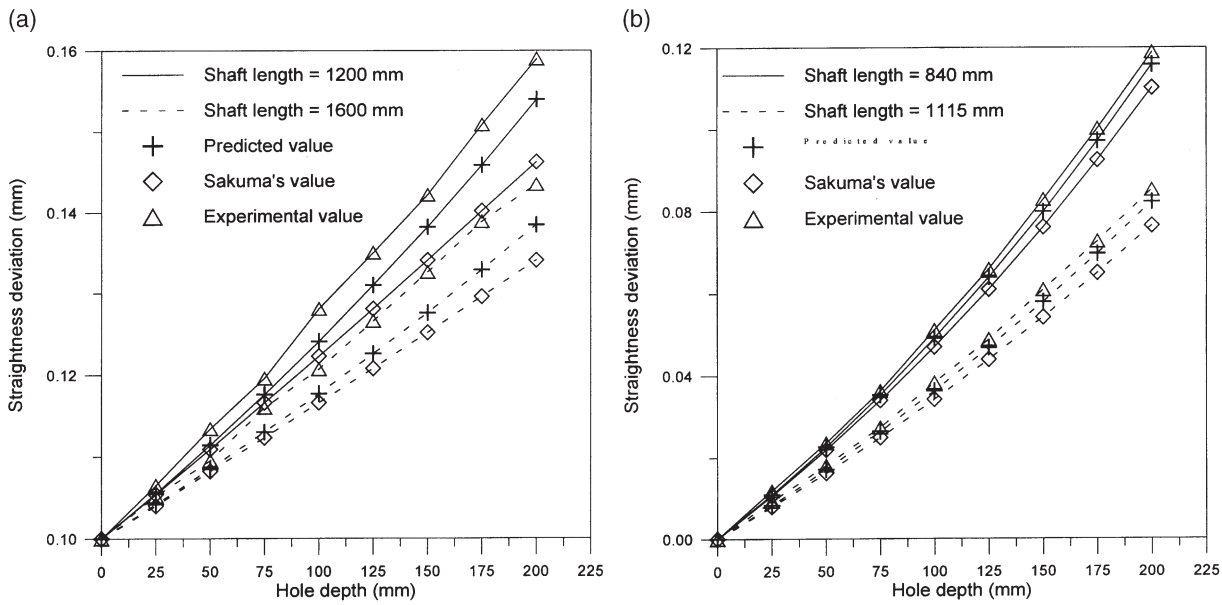

Fig. 9. (a) Influence of various BTA drilling shaft lengths on axial hole straightness deviation, feed rate: 0.05 mm/rev; pilot bushing misalignment: 0.1 mm; tool diameter: 18.91 mm. (b) Influence of various Gun drilling shaft lengths on axial hole straightness deviation, feed rate: 0.05 mm/rev; intermediate support misalignment: 0.1 mm; tool diameter: 12.52 mm.

with no intermediate support misalignment. The figure reveals that the straightness deflection increases with ℓ_1, a phenomenon that can be explained by Eq. (31), where the drill head slope i_0 is larger for a longer ℓ_1 than that for a short ℓ_1.

$$i_0=\frac{\delta_B}{L-\ell_1} \tag{31}$$

Fig. 11(b) displays the straightness deviation for intermediate support misalignment of 0.1 mm, with no pilot bushing misalignment. Here, a shorter ℓ_1 produced a larger straightness deflection. According to Castigliano's principle [14], this outcome can be explained by Eqs. (32a) and (32b), wherein the drill head slopes i_0 for shorter ℓ_1 are larger than for a longer ℓ_1, where R and Q denote, the positive reaction forces.

$$i_0=\frac{L^2}{2EI}\left(Q+\frac{R}{3}\right) \quad \text{for } \ell_1=\frac{L}{3} \tag{32a}$$

$$i_0=\frac{L^2Q}{2EI} \quad \text{for } \ell_1=\frac{L}{2} \tag{32b}$$

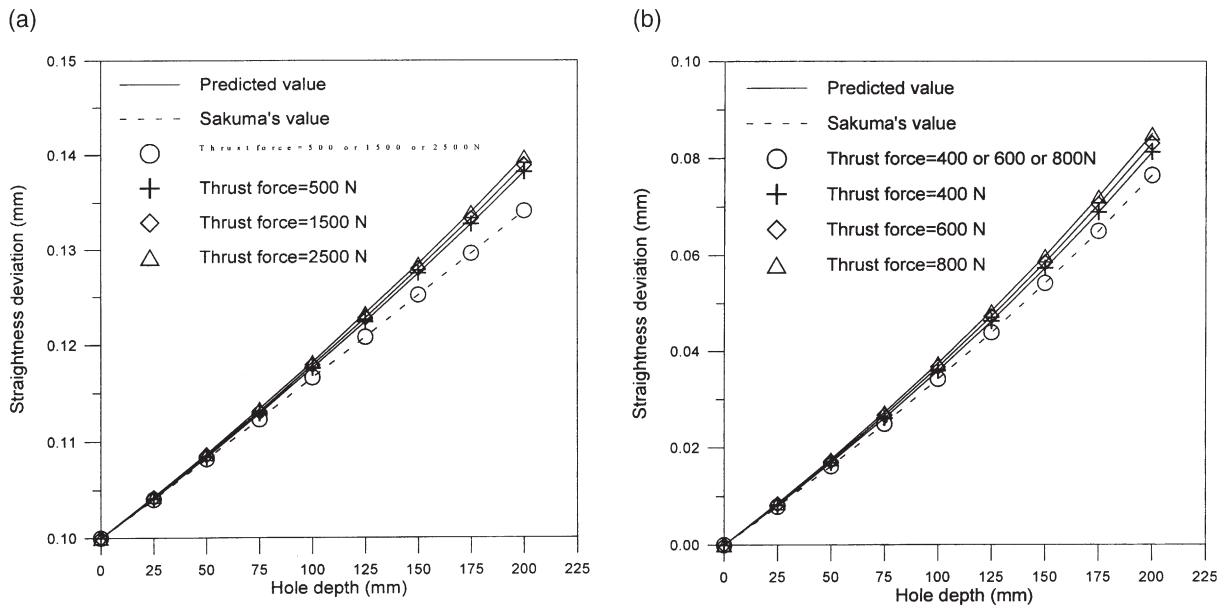

Fig. 10. (a) Influence of various BTA drilling thrust force on axial hole straightness deviation, pilot bushing misalignment: 0.1 mm; shaft length: 1600 mm; tool diameter: 18.91 mm; feed rate: 0.05 mm. (b) Influence of various Gun drilling thrust force on axial hole straightness deviation, intermediate support misalignment: 0.1 mm; shaft length: 1115 mm; tool diameter: 12.52 mm; feed rate: 0.05 mm.

4. Control factors analysis

4.1. Signal-to-noise ratios

A quality analysis to evaluate the conclusions obtained thus far is desirable. This analysis can be achieved by employing the S/N ratio to measure quality and orthogonal arrays and by simultaneously evaluating numerous parameters. Six control factors were used in the subsequent investigation: tool diameter; feed rate; shaft length; distance from spindle to intermediate support location; and misalignments in pilot bushing and intermediate support. Table 3(a) and (b) list the six control factors and the two selected levels. The levels were assigned randomly but limited by experiments. Employing the Taguchi method of parameter design, an L8 orthogonal array could provide the minimum seven degrees-of-freedom required in the experimental analysis, the basic L8 array had to be modified using the merging column method [16]. Further, a 2-level outer array was used to investigate the effect of the day-to-day variation (noise) of the drilling deep-hole process, and to provide an independent estimate of experimental error for assessing the main effects.

The S/N are derived from the quadratic loss functions [13]:

$$S/N = -10\log_{10}\left(\frac{1}{n}\sum_{i=1}^{n} y_i^2\right) \tag{33}$$

where n denotes the number of tests in a cell (in this study, n=4), and y_i represents the straightness

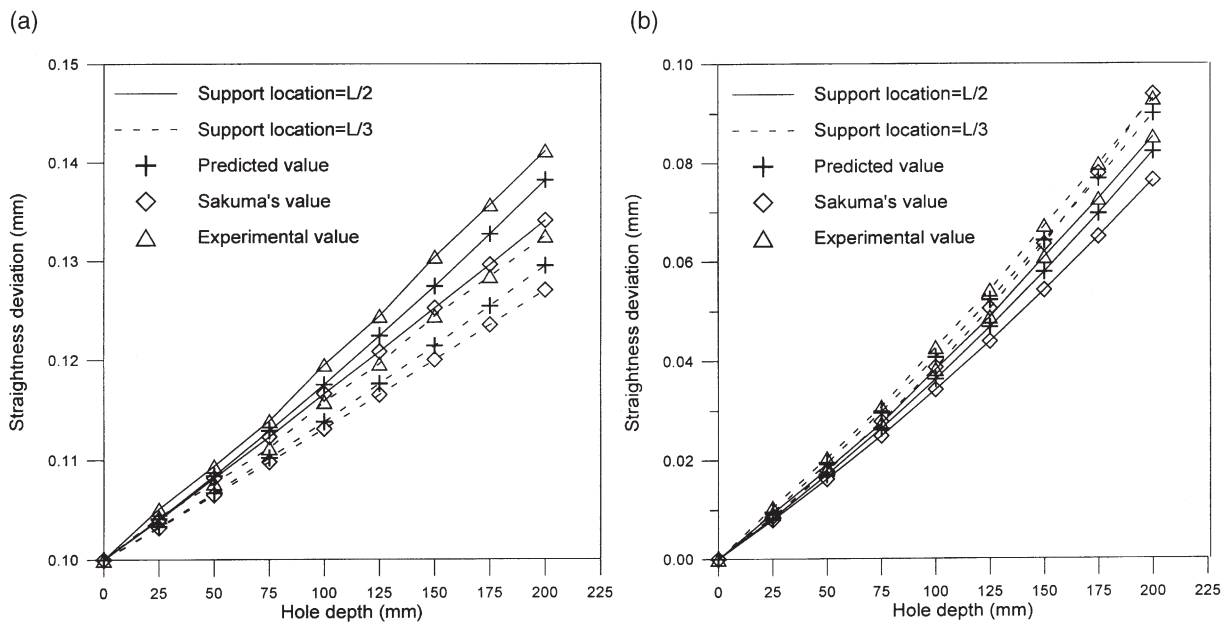

Fig. 11. (a) Influence of various BTA drilling intermediate support location on axial hole straightness deviation, feed rate: 0.05 mm/rev; pilot bushing misalignment: 0.1 mm; tool diameter: 26.40 mm; shaft length: 1600 mm. (b) Influence of various Gun drilling intermediate support location on axial hole straightness deviation, feed rate: 0.05 mm/rev; intermediate support misalignment: 0.1 mm; tool diameter: 12.52 mm; shaft length: 1115 mm.

deviation of tests in a cell. Table 4(a) and (b) list the S/N response ratios for the other characteristics obtained herein.

4.2. Analysis of variance

Analysis of variance (ANOVA) was carried out for the S/N ratios to determine the effects of the control factors. S/N optimization yielded high response and low variability, implying good cutting quality. Table 5(a) and (b) list the ANOVA for the S/N ratios corresponding to the hole straightness deviation function. The *F*-ratios and the percentage contributions for each process variable were also computed. ANOVA was carried out similarly on the S/N ratios of other quality characteristics.

4.3. Experimental interpretations

Fig. 12(a) and (b) plots the response graphs of the straightness deviation values against the six control factors and the thrust force. The highest average S/N ratio should be selected for the given process variables. The optimal combination of process variables was thus determined as $A_2B_1C_2D_1E_1F_1$. Meanwhile, for BTA drilling, the mean S/N ratio for the confirmatory experiment was predicted to be 20.19 dB with a 95% confidence band of ±0.560 dB. This predicted value was an improvement on the average S/N value of 18.83 dB obtained from the original settings of $A_1B_1C_1D_2E_1F_1$. The new combination achieved a gain of 1.36 dB, representing a 26.95%

Table 3
Factors and levels for the BTA drilling and Gun drilling experiments (cells in italic identify the starting levels)

Symbol	Factor	Level 1	Level 2
(a) *BTA drilling*			
A	Tool diameter (d)	*18.91 mm*	26.40 mm
B	Feed rate (ΔX)	*0.05 mm/rev*	0.1 mm
C	Tool length (L)	*1200 mm*	1600 mm
D	Distance from spindle to intermediate support location ()	L/3 mm	*L/2 mm*
E	Misalignment of pilot bushing (ℓ_1)	*0.05 mm*	0.1 mm
F	Misalignment of intermediate support (δ_B)	*0.05 mm*	0.1 mm
G ($A\times B$)	Thrust force (P)		
N	Day of the week (noise)	Day 1	Day 2
(b) *Gun drilling*			
A	Tool diameter (d)	*11.52 mm*	12.52 mm
B	Feed rate (ΔX)	0.05 mm/rev	0.1 mm
C	Tool length (L)	840 mm	1115 mm
D	Distance from spindle to intermediate support location (ℓ_1)	L/3 mm	L/2 mm
E	Misalignment of pilot bushing (δ_B)	0.05 mm	0.1 mm
F	Misalignment of intermediate support (δ_S)	0.05 mm	0.1 mm
G ($A\times B$)	Thrust force (P)		
N	Day of the week (noise)	Day 1	Day 2

reduction in axial hole straightness deviation. For Gun drilling, the predicted mean S/N ratio for the confirmatory experiment was 18.02 dB, with a 95% confidence band of ±0.740 dB. This predicted value was an improvement over the average S/N value of 16.38 dB obtained from the original settings of $A_1B_1C_1D_2E_1F_1$. The new combination achieved a gain of 1.64 dB, representing a 26.95% reduction in the axial hole straightness deviation.

4.4. Confirmatory experiments

In this series of experiments, eight samples were drilled at the levels of $A_2B_1C_2D_1E_1F_1$. For BTA drilling, the S/N results were 19.92 and 20.26 dB, representing an average value of 20.09 dB, within the 95% confidence band. For Gun drilling, the S/N results were 17.98 and 18.32 dB, representing an average value of 18.15 dB, again within the 95% confidence band. The optimum control factor settings were thus confirmed.

4.5. Discussions

S/N optimization yields a high response and low variability. Table 4 shows that a bigger tool diameter, 26.40 mm for BTA drilling and 12.52 mm for Gun drilling, was preferred in the parameter space explored herein. This effect could be because of the larger stiffness of the drill shaft that comes with the bigger tool diameter. A high feed rate would increase productivity, but a

Table 4
BTA drilling and Gun drilling experimental data

Trial no.	Factor and column no.						*N* (mm)		S/N (dB)
	A	B	C	D	E	F	Day 1	Day 2	
(a) *BTA drilling*									
1	1	1	1	1	1	1	0.109	0.113	19.09
2	1	1	1	2	2	2	0.227	0.231	12.80
3	1	2	2	1	1	2	0.130	0.126	17.85
4	1	2	2	2	2	1	0.166	0.170	15.49
5	2	1	2	1	2	1	0.160	0.157	15.97
6	2	1	2	2	1	2	0.120	0.124	18.27
7	2	2	1	1	2	2	0.220	0.217	13.17
8	2	2	1	2	1	1	0.113	0.117	18.78
(b) *Gun drilling*									
1	1	1	1	1	1	1	0.145	0.149	16.66
2	1	1	1	2	2	2	0.303	0.307	10.30
3	1	2	2	1	1	2	0.180	0.176	14.98
4	1	2	2	2	2	1	0.209	0.205	13.69
5	2	1	2	1	2	1	0.192	0.196	14.24
6	2	1	2	2	1	2	0.162	0.166	15.69
7	2	2	1	1	2	2	0.293	0.289	10.72
8	2	2	1	2	1	1	0.152	0.157	16.27

lower feed rate of 0.05 mm/rev was preferred in view of hole straightness, and this could be because of a lower axial thrust force (Eqs. (29a) and (29b)). Longer shaft length, of 1600 mm for BTA drilling and 1115 mm for Gun drilling was preferred in the experiments because the longer drill shaft has a smaller drill head slope i_0 (Eq. (30)). The distance from the spindle to the intermediate support location ℓ_1 of the tool shaft with the level 1 of (L/3) was preferred. Section 3.5 demonstrated that if the pilot bushing misalignment alone causes straightness deflection, then a longer ℓ_1 (Fig. 1) yielded a bigger hole deflection. Meanwhile, if the intermediate support misalignment alone causes straightness deflection, then a shorter ℓ_1 yielded a bigger hole deflection. Misalignments of pilot bushing and intermediate support proved important, and the lower support misalignment of 0.05 mm was prefered to the bigger support misalignment of 0.1 mm.

Table 5(a) and (b) illustrates the percentage contribution of various factors to the axial hole straightness deviation. The pilot bushing misalignment is the major factor, responsible for 79.76% of the BTA error and 65.71% of the Gun drilling error, followed by the intermediate support misalignment, with 15.05% for BTA drilling and 25.53% for Gun drilling. The axial thrust force and shaft lengths are less influential in hole deflection, 3.85% for BTA drilling and 6.31% for Gun drilling. Finally, tool diameter, feed rate and the distance from spindle to intermediate support location are together responsible for only a small portion of the deflection, totaling to 1.34% for BTA drilling and 2.45% for Gun drilling. To suppress the deflection and hence improve hole straightness, the assembly accuracy of pilot bushing, intermediate support and machine spindle influence are of primary importance.

Table 5
ANOVA of BTA drilling and Gun drilling full design (* indicates the sum of squares added together to estimate the pooled error sum ofthe squares indicated by parentheses; ** at least 99% confidence)

Symbol	DF	SS	V'	F	Effect	SS′	P
(a) *BTA drilling*							
A	1	0.120*			**		
B	1	0.084*			**		
C	1	1.730	1.730	33.9	**	1.648	3.85
D	1	0.072*			**		
E	1	34.197	34.197	670.5	**	34.115	79.76
F	1	6.516	6.516	127.7	**	6.434	15.05
G	1	1.730	1.730	33.9	**	1.648	3.85
($A\times B$)							
Error	1	0.051*					
Error (pooled)	(4)	(0.327)	(0.082)			(0.573)	(1.34)
Total	7	42.770				42.770	100
(a) *Gun drilling*							
A	1	0.208*			**		
B	1	0.189*			**		
C	1	2.703	2.703	19.0	**	2.561	6.31
D	1	0.053*			**		
E	1	26.828	26.828	188.9	**	26.686	65.71
F	1	10.511	10.511	74.0	**	10.369	25.53
G	1	2.703	2.703	19.0	**	2.561	6.31
($A\times B$)							
Error	1	0.117*					
Error (pooled)	(4)	(0.567)	(0.142)			(0.993)	(2.45)
Total	7	40.609				40.609	100

5. Conclusions

Deep-hole drilling is known for its good hole quality, including good hole straightness. However, this quality can be easily ruined by inaccurate machine assembly. The present study investigated hole straightness deviations using the Euler column theory. In deep-hole drilling, hole straightness deviations are affected by tool diameter, feed rate, shaft length, distance from spindle to intermediate support location, and misalignments of pilot bushing and intermediate support. This paper investigated hole deflections in an environment that includes misalignments in the pilot bushing or intermediate supports of the drill shaft. Application of statistical techniques such as Taguchi's parameter designs and ANOVA lead to objective and quantitative conclusions, and these conclusions are analyzed herein. The findings can be summarized as follows:

1. Interestingly, for both BTA and Gun drilling, the shorter drill shaft yielded bigger straightness deflection.
2. In deep-hole drilling, thrust applied to drill shafts softened the effective stiffness of the shafts.

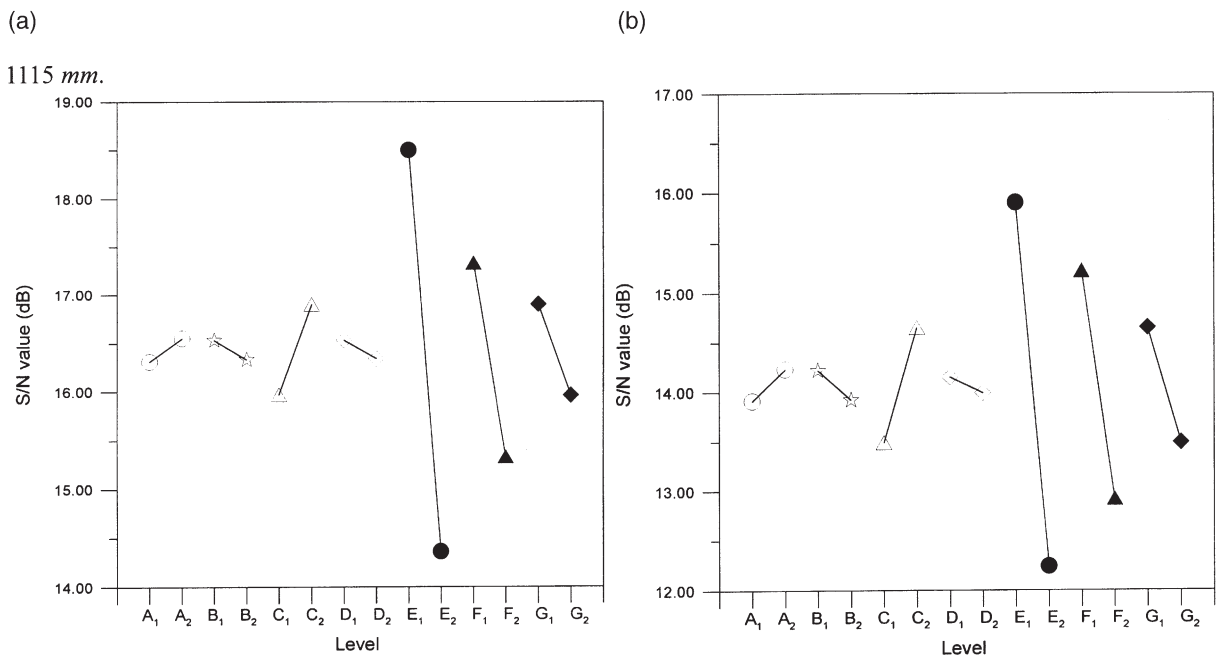

Fig. 12. (a) Response graphs of BTA drilling. (b) Response graphs of Gun drilling.

Sakuma's model did not consider the thrust force, and hence could not properly predict the hole straightness deviations.

3. If the pilot bushing misalignment alone causes straightness deflection, then longer ℓ_1 yields bigger straightness deflection. Meanwhile, if the intermediate support misalignment alone causes straightness deflection, then shorter ℓ_1 yields bigger straightness deflection.
4. The parameters make different percentage contributions to the hole straightness deviation. The pilot bushing misalignment contributes a greatest percentage of 79.76% for BTA drilling and 65.71% for Gun drilling, followed by the intermediate support misalignment of 15.05% for BTA drilling and 25.53% for Gun drilling. Next, the axial thrust force and shaft lengths are responsible for 3.85% for BTA drilling and 6.31% for Gun drilling. Finally, tool diameter, feed rate and the distance from spindle to intermediate support location together account for only a small portion of hole straightness deviation, totaling to 1.34% for BTA drilling and 2.45% Gun drilling. Hole straightness deviation is thus most heavily influenced by the pilot bushing and intermediate support misalignments. To suppress the deflection and hence improve hole straightness, the assembly accuracy of pilot bushing, intermediate support and machine spindle influence are most important.
5. Optimum control factor settings of $A_2B_1C_2D_1E_1F_1$ were found to yield lower axial hole straightness deviation, with the predicted response confirmed experimentally. Compared to the original settings of $A_1B_1C_2D_2E_1F_1$, a reduction of 26.95% in hole straightness deviation is obtained for BTA drilling, and 31.54% for Gun drilling.
6. Comparison between the simulated and experimental results showed that the column equation, despite its apparent simplicity, adequately describes the phenomenon of a deep-hole drill shaft subjected to thrust in drilling.

Acknowledgements

The authors would like to thank the National Science Council of the People's Republic of China for financially supporting this research under the Contract No. NSC-87-2212-E-009-024.

Appendix A

Experimental equipment:

1. Lathe
   SAN SHING SK26120 HEAVY DUTY PRECISION LATHE
   BTA drilling system (Fig. 6(a))
   Gun drilling system (Fig. 6(b))
2. BTA drilling
   (a) Tool head: SANDVIK 420.6 series
   (b) Drill shaft
   Type: SANDVIK 420.5-800-2
   - Tool head: 18.91 and 19.90 mm, internal and external diameters of drill shaft: 11.5 and 17 mm, respectively
   - Tool head: 24.11 and 26.40 mm, internal and external diameters of drill shaft: 14 and 22 mm, respectively

   Material: JIS SNCM 21
   Density ρ: 7850 kg/m^3
   Young's modulus E: 206×10^9 Pa
3. Gun drilling
   Type: ELDORADO series
   Material: JIS SCM 3
   Density ρ: 7850 kg/m^3
   Young's modulus E: 205×10^9 Pa
4. Cutting Fluid
   Type: R32
   Density ρ_f: 871 kg/m^3
   Absolute viscosity μ: 0.383 kg/m s
5. Dynamometer
   Model: 6423-3K S/N 140
   Rated capacity (compression only): 3000 lb
   Maximum load (without zero shift): 50% overload (150% of rated capacity)
   Signal sensors: Four arm bonded strain gauge bridges

Appendix B

Axial hole deviation equations derived by Sakuma

(a) With pilot bushing misalignment, no intermediate support

$$e_n=\left(1+\frac{3}{2L}\Delta X\right)^n\delta_B \tag{B1}$$

(b) With intermediate support misalignment, no pilot bushing deviation at the beginning of drilling; inclination i_n of the tool head axis at penetration length X_n, is given by:

$$i_n=\frac{1}{2A}\left\{\frac{[2L^2(\ell_1-X_n)-A](3Ae_n+6\delta_S L^3)}{(\ell_1-X_n)\left\{2L^3-\left[1+\frac{3(\ell_2+X_n)}{2(\ell_1-X_n)}\right]A\right\}}-6\delta_S L^2\right\} \tag{B2}$$

where $A=2L^3-2L^2(\ell_2+X_n)+(\ell_2+X_n)^3$.

References

[1] J. Frazao, S. Chandrashekhar, M.O.M. Osman, T.S. Sankar, On the design and development of a new BTA tool to increase productivity and workpiece accuracy in deep-hole machining, The International Journal of Advanced Manufacturing Technology 4 (1986) 3–23.

[2] K. Sakuma, K. Taguchi, A. Katsuki, Study on deep-hole-drilling with solid-boring tool — the burnishing action of guide pads and their influence on hole accuracies, Bulletin of the JSME 23 (1980) 1921–1928.

[3] K. Sakuma, K. Taguchi, A. Katsuki, Study on deep-hole-drilling boring by bta system solid-boring tool — behavior of tool and its effect on profile of machined hole, Bulletin of the Japan Society of Precision Engineering 14 (1980) 143–148.

[4] K. Sakuma, K. Taguchi, A. Katsuki, Self-guiding action of deep-hole-drilling tools, Annals of the CRIP 30 (1981) 311–315.

[5] P.K. Rao, M.S. Shunmugam, Analysis of axial and transverse profiles of holes obtained in BTA machining, International Journal of Machine Tool and Manufacture 27 (1986) 505–515.

[6] A. Katsuki, K. Sakuma, K. Taguchi, H. Onikura, H. Akiyoshi, Y. Nakamuta, The influence of tool geometry on axial hole deviation in deep drilling: comparison of single- and multi-edge tools, JSME International Journal 30 (1987) 1167–1174.

[7] A. Katsuki, H. Onikura, H.K. Sakuma, T. Chen, Y. Murakami, The influence of workpiece geometry on axial hole deviation in deep-hole drilling, JSME International Journal 35 (1992) 160–167.

[8] H.O. Stuerenburg, Zum Mittenverlauf beim Tiefbohren, Dissertation, University of Stuttgart, 1983.

[9] Y.A. Youssef, Y. Beauchamp, M. Theomas, Comparison of a full factorial experiment to fractional and Taguchi designs in a lathe day turning operation, Computers and Industrial Engineering 27 (1994) 59–62.

[10] S.C. Tam, L.E.N. Lim, K.Y. Quek, Application of Taguchi methods in the optimization of the laser-cutting process, Journal of Materials Processing Technology 29 (1992) 63–74.

[11] Y.V. Hui, L.C. Leung, Optimal economic tool regrinding with Taguchi's quality loss function, The Engineering Economist 39 (1994) 313–331.

[12] Y.L. Su, S.H. Yao, C.S. Wei, C.T. Wu, Analyses and design of a WC milling cutter with TiCN coating, Wear 215 (1998) 59–66.

[13] G. Taguchi, System of Experimental Design, vols. 1–2, American Supplier Institute Inc, 1987.

[14] N.R. Bauld, Mechanics of Materials, 1st ed., Wadsworth Inc., Monterey, CA, 1982.

[15] Y.L. Perng, J.H. Chin, Theoretical and experimental investigations on the spinning BTA deep-hole drill shafts containing fluids and subject to axial forces, International Journal of Mechanical Sciences 41 (1999) 1301–1322.
[16] M.S. Phadke, Quality Engineering Using Robust Design, Prentice Hall, Englewood Cliffs, NJ, 1989.